

Vietnam Journal of Chemistry, International Edition, **55**(4): 438-445, 2017  
DOI: 10.15625/2525-2321.2017-00487

## A quantum chemical computation insight into the donor-acceptor bond interaction of silver complexes with tetrylene

Tran Duc Sy<sup>1,5</sup>, Huynh Thi Phuong Loan<sup>2</sup>, Dang Tan Hiep<sup>3</sup>,  
Pham Van Tat<sup>4</sup>, Duong Tuan Quang<sup>5</sup>, Nguyen Thi Ai Nhung<sup>2\*</sup>

<sup>1</sup>Department of Chemistry, Quang Binh University

<sup>2</sup>Department of Chemistry, Hue University of Sciences, Hue University

<sup>3</sup>HCMC University of Food Industry,

<sup>4</sup>Faculty of Science and Technology, Hoa Sen University

<sup>5</sup>Department of Chemistry, Hue University of Education, Hue University

Received 11 February 2017; Accepted for publication 28 August 2017

### Abstract

We computationally investigate the nature of chemical bonding from linear to bent structures of N-heterocyclic carbene-analogues of silver complexes (called tetrylene)  $\text{AgCl-NHE}_{\text{Me}}$  (**Ag-NHE**) with  $\text{E} = \text{C} - \text{Pb}$  using quantum chemical calculations at the BP86 level with the various basis sets def2-SVP, def2-TZVPP, and TZ2P+. The geometry calculations find that the equilibrium structures of **Ag-NHE** system show major differences in the bonded orientation of **NHPb** ligand in **Ag-NHPb** compared with **NHE** ligands the slighter homologues **Ag-NHE** ( $\text{E} = \text{C} - \text{Sn}$ ). The bond dissociation energy results show that the Ag-carbene bond in **Ag-NHC** is a strong bond and decreases from the slighter to the heavier homologues. The EDA-NOCV results indicate that the ligand **NHE** in complexes is strong  $\sigma$ -donors and very weak  $\pi$  donor. The NOCV pairs of the bonding show small  $\pi$ -back donation from the Ag to the  $\text{NHE}_{\text{Me}}$  ligands.

**Keywords.** N-heterocyclic tetrylene, bond dissociation energy, quantum chemical calculations, bonding analysis.

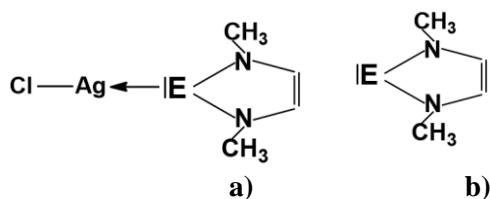
### 1. INTRODUCTION

The first stable transition metal carbene complex was investigated in 1964 [1]; then the metal-ligand bonding in complexes of mixed carbene-halogen complexes (NHC-TMX with  $\text{TM} = \text{Cu}, \text{Ag}, \text{Au}$  and  $\text{X} = \text{F} - \text{I}$ ) was published for using a charge decomposition analysis that was noticed for the first time by Frenking et al [2]. The chemical bonding between NHCs and group 11 metals has been investigated theoretically in the recent past [3]. Moreover, NHCs ligands can be stabilized by two nitrogen atoms and form stable complexes with transition metals (Ag, Au) and with main-group elements [2]. The fact was that silver-NHCs complexes have been investigated in the recent past to behave as efficient catalysts in transesterification reactions [4]. Furthermore, silver-NHCs compounds are the most popular complexes used for NHCs transfer [5]. The development of NHCs complexes of silver has come about by the discovery of the transmetalation from silver-NHCs to other metal NHCs system. Unlike copper- and gold-NHCs

systems, silver-NHCs can be synthesized without the need for anaerobic conditions [6] that has been shown in many biomedical applications within the last ten years. For example, in 2007 Youngs et al. [7] reviewed the synthesis, characterization, and applications of silver(I)-NHCs complexes for antibiotics applications. We especially pay attention to the use of metal-NHCs complexes as precursors for the synthesis of nanocrystals in which very few reports refer to syntheses and stabilization of metal nanocrystals through gold- and silver-NHCs complexes [8,9]. It has been known that the steric bulk of the NHC and the strength of the reducing agent were found to have an interesting influence on nanocrystals size, size contribution, and shape of the metal-NHCs adducts [10]. The formation of silver nanoparticles from the reduction of silver-NHCs complexes with the  $\text{C}_n\text{H}_{2n+1}$  groups connected to nitrogen atoms in NHC ring that was also observed by  $\text{NaBH}_4$  in biphasic conditions ( $\text{CH}_2\text{Cl}_2/\text{H}_2\text{O}$ ) [11]. Recent reports suggested that the characterization and the bonding situation in transition metal complexes with NHCs ligands [12] and related

systems [13] are not limited to carbon as a central atom, but that is can be extended to the heavier group 14 homologues that have been extensively investigated in the recent past [2,14,15].

Our interest lies in having a thorough insight into the structures and bonding situation of silver-NHC<sub>Me</sub> and analogues [AgCl- $\{NHE_{Me}\}$ ] (**Ag-NHE**) complexes with E = C – Pb. In this regard, we have recently reported and also have employed in a variety of a series of [AuCl- $\{NHE_{Me}\}$ ] complexes [15]. During the course of the investigation of the silver complexes that carry tetrylene we became interested in looking for the existence of silver(I)-NHC<sub>Me</sub> complexes that have been previously used as precursors for the synthesis of nanocrystals [11]. To the best of our knowledge, the present work is the first detailed study of the structures and bonding situation of the complexes **Ag-NHE** (Scheme 1). We investigated the bonding in complexes **Ag-NHE** and the electronic structure of the molecules was analyzed with charge- and energy decomposition methods. A schematic representation of the bonding in AgCl←NHE<sub>Me</sub> with  $\sigma$ -donors and  $\pi$ -donors of interactions is suggested. We hope that the information of bonding in complexes **Ag-NHE** is suitable targets for synthesis.



*Scheme 1:* Overview of the compounds investigated in the present work: a) Complexes [AgCl- $\{NHE_{Me}\}$ ] (**Ag-NHE**) and b) Ligand NHE<sub>Me</sub> (**NHE**) with E = C – Pb

## 2. COMPUTATIONAL METHODS

Geometry optimizations of the molecules were carried out without symmetry constraints using Gaussian 09 optimizer together with Turbomole 7.0 energies and gradients at the BP86/def2-SVP level of theory. Single point calculations with the same functional but the larger def2-TZVPP basis set and effective core potentials (ECPs) were examined to represent the innermost electrons of Ag atom as well as the electrons core of the heavier group-14 atoms Sn and Pb on the structures derived on BP86/SVP level of theory. The natural bond orbital (NBO) analysis was carried out with the internal module of Gaussian 09 at the BP86/def2-TZVPP//BP86/def2-SVP level of theory. For bonding analysis in term of energy decomposition analysis, the geometries of the

molecules were re- optimized with the program package ADF 2013.01 with BP86 in conjunction with a triple-zeta-quality basis set using uncontracted Slater-type orbitals (STOs) augmented by two sets of polarization function, with a frozen-core approximation for the core electrons. An auxiliary set of *s*, *p*, *d*, *f* and *g* STOs were used to fit the molecular densities and to represent the Coulomb and exchange potentials accurately in each SCF cycle. Scalar relativistic effects were incorporated by applying the zeroth-order regular approximation (ZORA). The calculations have been carried out at the BP86/TZ2P+ level of theory that was used for the bonding analyses in term of the EDA – NOCV method.

## 3. RESULTS AND DISCUSSION

### 3.1. Structures and energies

Figure 1 shows the optimized geometries of the parent compounds **Ag-NHC**–**Ag-NHPb** at the BP86/SVP level together with the most important bond lengths, bending angles, and bond dissociation energies (BDEs). There are no experimental values available for the complexes **Ag-NHC** to **Ag-NHPb**. The theoretically predicted Ag-E bond length of **Ag-NHE** complexes increased from 2.058 to 2.773 Å. The fact was that the related complexes of N-heterocyclic carbene and slightly heavier homologues (NHE<sub>Me</sub> and NHE<sub>H</sub> with E = C, Si, Ge) such as gold(I) chloride AuCl and copper(I) chloride CuCl were theoretically investigated in the recent past [15, 16]. The results showed that the theoretically predicted Au-E bond lengths of complexes AuCl-NHE<sub>Me</sub> with E = C – Pb as AuCl-NHC<sub>Me</sub> = 1.997 to AuCl-NHPb<sub>Me</sub> = 2.708 Å [15]; the bond lengths Au-E of complexes AuCl-NHE with E = C – Ge as AuCl-NHC<sub>H</sub> = 1.976 to AuCl-NHGe<sub>H</sub> = 2.349 Å [16] and the bond lengths Cu-E of complexes CuCl-NHE with E = C – Ge as CuCl-NHC<sub>H</sub> = 1.848 to CuCl-NHGe<sub>H</sub> = 2.250 Å reported in the previous study [16] are slightly shorter than the bond lengths Ag-E of **Ag-NHE** complexes in this study. Moreover, we want to compare the theoretically predicted Ag-E bond lengths of the tetrylene complexes **Ag-NHC** to **Ag-NHGe** with some experimental results of the related complexes. In general, the theoretically predicted Ag-E bond lengths of **Ag-NHE** in this study are shorter than the experimental results measured Ag-E bonds of carbene-analogues complexes [17-20]. For example, the carbene complex NHC-AgCl has C-Ag lengths in the range 2.061 Å [17], which is longer than the C-Ag bond length in the carbene complex **Ag-NHC**

(2.058 Å). The silylene complex  $(R^H_2Si)_2Ag$  with  $R = 1,1,4,4$ -tetrakis(trimethylsilyl)butane-1,4-diyl [18], as a bicyclic silylene ligand, has Ag-Si bond length of 2.401 Å whereas the Ag-Si bond in the silylene complex **Ag-NHSi** has a length of 2.317 Å. The  $\{LGe[C(SiMe_3)N_2]AgC_6F_5\}$  ( $L = HC[C(Me)N-2,6-iPr_2C_6H_3]_2$ ) [19] has an experimental Ag-Ge bond length of 2.448 Å, which is also longer than the Ag-Ge bond in **Ag-NHGe** (2.404 Å). However, the bond length Ag-Sn of complex  $[(Ag(SCN)\{Sn(CHR_2)_2\}-(OC_4H_8)_2)_2]$  is 2.598 Å [20] shorter than the stannylyene adduct **Ag-NHSn** has Ag-Sn = 2.602 Å. Figure 1 also shows that the examination of the equilibrium geometries of **Ag-NHC–Ag-NHPb** shows tetrylene ligands **NHE** are bonded end-on way to AgCl in the complexes **Ag-NHE** ( $E = C - Sn$ ) which is the bending angle,  $\alpha$ , which is  $180.0^\circ$ , while the ligand plumbylene in **Ag-NHPb** is bonded in a side-on fashion, which is the bending angle,  $\alpha$ , is  $85.0^\circ$ . Figure 1 gives the theoretically predicted BDEs for Ag-E bonds of **Ag-NHC–Ag-NHPb**, which exhibit an interesting trend. The calculated bond energies suggest that the Ag-tetrylene ligands bond strength decrease from **Ag-NHC** ( $D_e = 57.3$  kcal/mol) to **Ag-NHSi** ( $D_e = 45.2$  kcal/mol). There is a continuous strengthening of the BDEs for the

heavier ligands from **Ag-NHSi** ( $D_e = 45.2$  kcal/mol) to **Ag-NHPb** ( $D_e = 28.6$  kcal/mol). The trend of the theoretically predicted AgCl-tetrylenes BDEs in this study is significantly lower than the calculated values for the gold(I) chloride AuCl complexes that carry tetrylene ligands ( $AuCl-NHC_{Me} - AuCl-NHPb_{Me}$ ) with the BDEs change from  $D_e = 79.2$  to 42.7 kcal/mol [15]; and for the gold(I) chloride AuCl complexes that carry the less bulky slighter tetrylene ligands ( $AuCl-NHC_H - AuCl-NHGe_H$ ) with the BDEs change from  $D_e = 82.8$  to 49.4 kcal/mol [16]; and with the copper(I) chloride CuCl complexes that carry the less bulky slighter tetrylene ligands ( $CuCl-NHC_H - CuCl-NHGe_H$ ), the BDEs decrease from  $D_e = 67.4$  to 35.1 kcal/mol [16]. The bond length Ag-E of the complexes **Ag-NHE** was longer than the bond Au-E and Cu-E of the complexes gold-tetrylene [15,16] and copper-tetrylene [16]. This is quite suitable because the metal-NHE<sub>Me</sub> interactions of NHE<sub>Me</sub>-AgCl have small NHE<sub>Me</sub>←AgCl  $\pi$ -back-donation in complexes. From this, it follows that the silver donor-acceptor complexes with carbene, silylene, and germylene ligands can have very strong bonds and the appearance of a small contribution in free ligands←AgCl  $\pi$ -back-donation in complexes which will be further explained in bonding analysis.

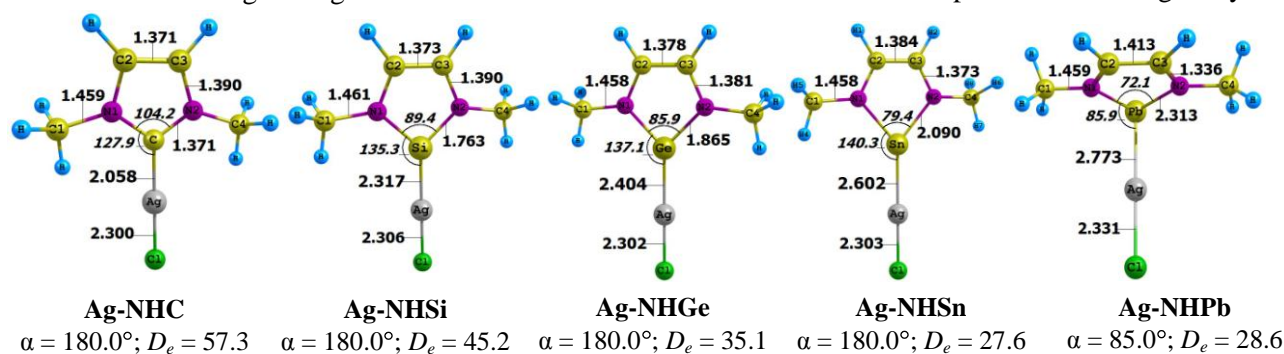
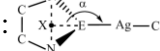


Figure 1: Optimized geometries of complexes **Ag-NHC–Ag-NHPb** at the BP86/def2-SVP level. Bond lengths are given in Å; angles in degrees. Calculated bond dissociation energy,  $D_e$  (kcal/mol), for the ligand-AgCl bonds in complexes at the BP86/def2-TZVPP//BP86/def2-SVP level. The bending angles,  $\alpha$ , are the angles X-E-Ag where X is the midpoint between the N-N distances:



### 3.2. BONDING ANALYSIS

Table 1 gives results of the NBO calculations for parent compounds **Ag-NHC–Ag-NHPb**. The calculated partial charges show that the AgCl fragment in the complexes always carries a negative charge, which increases from **Ag-NHC** (-0.28 e) to **Ag-NHPb** (-0.37 e), except the value of **Ag-NHSi** is -0.37 e. The Wiberg bond orders for the Ag-E bond in **Ag-NHE** increases from **Ag-NHC** (0.59) to **Ag-NHSi** (0.77), but then decreases from **Ag-NHSi** to

**Ag-NHPb** (0.44). We would like to comment on the partial atomic charges of the donor atoms E and the acceptor atom Ag in the complexes **Ag-NHE**. The silver atom always carries a positive charge between 0.21 e ( $E = Si$ ) and 0.31 e ( $E = C$ ). The carbon donor atom in **Ag-NHC** has a small positive charge of 0.11 e while the heavier atoms have a large positive charge between 0.75 e ( $E = Pb$ ) and 1.08 e ( $E = Si$ ). The unusually smallest Wiberg bond order value of Ag-C bond in complex **Ag-NHC** can be explained by the shortest bond length and possibly due to the

shortest Ag-C bond length with the more bulky substituent CH<sub>3</sub> groups in the NHE<sub>Me</sub> moieties of the tetrylene ligands. Note that the partial charge value of AgCl in complex **Ag-NHSi** also exhibits the large negatively charge (-0.37 e). We realize that the trend

of the partial charges does not support the suggestion that there is a change from ligand donation [Ag]→NHE<sub>Me</sub> for the head-on bonded lighter homologues to metal donation [Ag]→NHE<sub>Me</sub> for the side-on bonded adduct.

*Table 1:* NBO results with Wiberg bond indices (WBI) and natural population analysis (NPA) at the BP86/def2-TZVPP//BP86/def2-SVP level for complexes **Ag-NHC–Ag-NHPb**. The partial charges, *q*, are given in electrons [e]

Molecule	Bond	WBI	<i>q</i> [AgCl]	Atom	NPA ( <i>q</i> )
<b>Ag-NHC</b>	Ag-C	0.59	-0.28	Ag	0.31
	C-N1	1.27		C	0.11
	C-N2	1.27		N	-0.31
	Ag-Cl	0.65		Cl	-0.59
<b>Ag-NHSi</b>	Ag-Si	0.77	-0.37	Ag	0.21
	Si-N1	0.83		Si	1.08
	Si-N2	0.83		N	-0.70
	Ag-Cl	0.65		Cl	-0.58
<b>Ag-NHGe</b>	Ag-Ge	0.63	-0.30	Ag	0.27
	Ge-N1	0.80		Ge	0.99
	Ge-N2	0.80		N	-0.68
	Ag-Cl	0.66		Cl	-0.57
<b>Ag-NHSn</b>	Ag-Sn	0.57	-0.31	Ag	0.26
	Sn -N1	0.73		Sn	1.01
	Sn -N2	0.73		N	-0.66
	Ag-Cl	0.67		Cl	-0.57
<b>Ag-NHPb</b>	Ag-Pb	0.44	-0.37	Ag	0.23
	Pb-N1	0.57		Pb	0.75
	Pb-N2	0.57		N	-0.54
	Ag-Cl	0.60		Cl	-0.61

As pointed out in the computational details, the molecules have C<sub>1</sub> symmetry with no genuine  $\sigma$  and  $\pi$  orbitals since there is no mirror plane in the molecular structure. We consider the strength of the  $\pi$  donation NHE<sub>Me</sub>→AgCl which may be expected from the  $\sigma$ - and  $\pi$  lone-pair orbital of the ligand NHE<sub>Me</sub> into the second vacant coordination side of metal fragment AgCl, we have to keep visually the shapes of **Ag-NHPb** in one plane to identify  $\sigma$ - and  $\pi$ -type molecular orbitals. Figure 2 shows two occupied molecular orbitals and orbital energies of  $\sigma$ -type and  $\pi$ -type MOs from **Ag-NHC–Ag-NHPb** at the BP86/TZVPP level. The energy level of the  $\pi$ -type donor orbital of **Ag-NHSi–Ag-NHPb** is higher lying than the  $\sigma$ -type donor orbital whereas the energy level of the  $\pi$ -type donor orbital from **Ag-NHC** is lower lying than the  $\sigma$ -type donor orbital. Note that the shape of the  $\sigma$ - and  $\pi$ -orbitals (HOMO-11 and HOMO-10) of complex **Ag-NHPb** is significantly different from the shapes of the slighter homologues Ag-NHE (E = C – Sn). This can be explained by a detailed insight into the bonding situation of the side-on bonded plumblylene **Ag-**

**NHPb** where the bending angle  $\alpha$  is bonded in the strongest side-on mode ( $\alpha = 85.0^\circ$ ). Especially, the shape of the molecular orbitals indicates that NHE<sub>Me</sub>→AgCl not only has significant  $\sigma$  donation but also exhibits a bit  $\pi$  donation in complexes. We can explain that the  $\pi$  donation in complexes is due to the strong N→E  $\pi$  donation at the ring of the NHE<sub>Me</sub> ligands.

We want to point out that the orbitals at the Ag side carry a little NHE<sub>Me</sub>←AuCl back-donation and mainly exhibit NHE<sub>Me</sub>→AuCl  $\sigma$ -donation. We suggest the Scheme 2 with the Scheme 2 (d) firstly shows an orbital diagram of N-heterocyclic carbenes and analogues and bonds of NHE to Ag center. We realize that the nitrogen in the ring NHE<sub>Me</sub> can act as ligands which indicate N→E donation and the NHE<sub>Me</sub> ligands have the resonance form for molecules which exhibits the orbital overlap between the  $\pi$ -type lone pair and the N-E  $\pi^*$ -orbitals which exhibits in more electron density at E atom which is shown in Scheme 2 (a) and Scheme 2 (b). Furthermore, Scheme 3 also shows that N-heterocyclic tetrylene NHE<sub>Me</sub> in which the central E

atom can have two lone pairs may show the characteristics of an E(0) compounds with E = C, Si, Ge, Sn, Pb (Scheme 2 (b)). The resonance form may be ignored due to the  $\pi$ -type lone pair is delocalized;

this leads to the loss of aromaticity. Moreover, Schemes 2 (b, c, d) also exhibit a back-donation from metal fragment to E atom of ligand tetrylene.

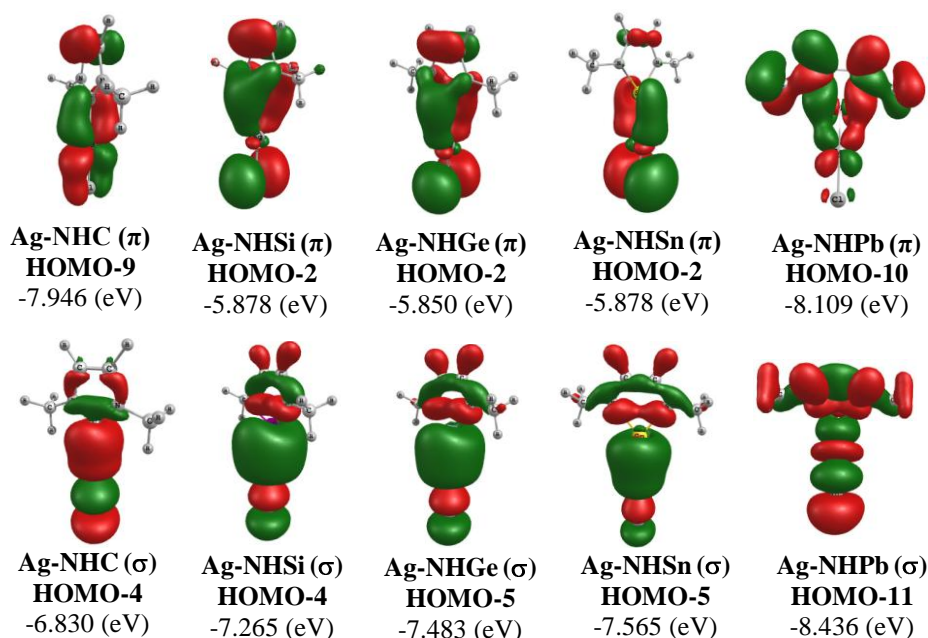
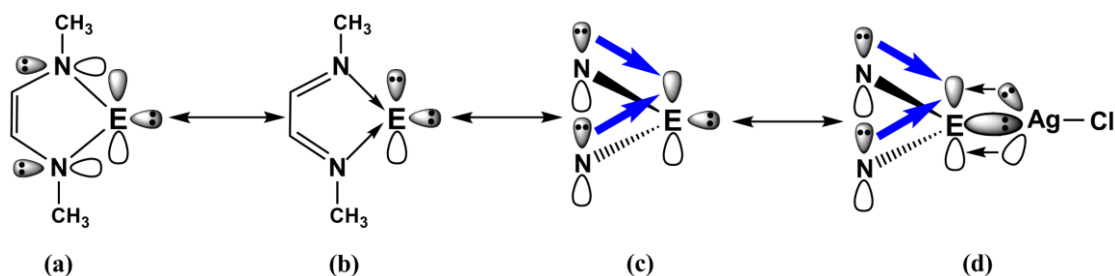


Figure 2: Molecular orbitals and orbital energies of  $\sigma$ -type and  $\pi$ -type in **Ag-NHC–Ag-NHPb** at the BP86/def2-TZVPP level. Orbital energies are given in eV



Scheme 2: Suggested schematic representation of  $\text{NHE}_{\text{Me}}$  showing: a) Divalent element E(II) character (tetrylenes); b) Divalent element E(0) character with the 2 lone pairs at E atom; b) and c) Correspondent possible resonance forms of element E(II) and element E(0) ligands showing the divalent element E(II) and the divalent element E(0) characters with E = C – Pb; d) Bonding of  $\text{NHE}_{\text{Me}}$  ligand to metal fragment AgCl

In order to give a detailed insight into the bonding situation of complexes, we analyzed the nature of the donor-acceptor interactions in **Ag-NHE** with the EDA in conjunction with the NOCV method. Table 2 gives the numerical results of the **Ag-NHE** interactions at the BP86/TZ2P+ level. The trend of the bond dissociations energies (BDEs),  $\Delta E$  ( $= -D_e$ ) [kcal/mol], for the Ag-E bond in **Ag-NHE** system decrease from the lighter to the heavier homologues (**Ag-NHC**:  $-D_e = -55.0$  kcal/mol; **Ag-NHPb**:  $-D_e = -27.5$  kcal/mol). The decrease of the BDEs from the lighter to heavier adduct is determined by the intrinsic strength of the metal-ligand bonds  $\Delta E_{\text{int}}$  in which the intrinsic energy  $\Delta E_{\text{int}}$

values decreases from -55.7 kcal/mol (**Ag-NHC**) to -29.5 kcal/mol (**Ag-NHPb**) of the system. The preparation energy  $\Delta E_{\text{prep}}$  of complexes changes from 0.7 in **Ag-NHC** to 2.0 kcal/mol in **Ag-NHPb**. The three main terms Pauli repulsion  $\Delta E_{\text{Pauli}}$ , electrostatic interaction  $\Delta E_{\text{elstat}}$ , and orbital interaction  $\Delta E_{\text{orb}}$  are considered to inspect their contribution to the intrinsic energy  $\Delta E_{\text{int}}$  of the complexes. Inspection of the three main terms indicated that the Pauli repulsion  $\Delta E_{\text{Pauli}}$  has the largest value of 132.7 kcal/mol for **Ag-NHC** and gets smaller from E = C to E = Pb (48.0 kcal/mol). We realized that the decrease of the BDEs from the

lighter to heavier adduct is determined by the electrostatic strength of the metal-ligand bonds  $\Delta E_{elstat}$ . The electrostatic strength  $\Delta E_{elstat}$  of **Ag-NHE** decreases from **Ag-NHC** (-146.2 kcal/mol) to **Ag-NHSi** (-119.9 kcal/mol), then **Ag-NHGe** (-79.2 kcal/mol), **Ag-NHSn** (-59.7 kcal/mol), and then **Ag-NHC** (-45.3 kcal/mol). Table 2 also shows that the

contribution of  $\Delta E_{\sigma}$  to  $\Delta E_{orb}$  was rather large for all complexes where the values were between 65.5 – 85.5 %. Thus, the EDA-NOCV calculations show that the Ag-E bonding in the complexes **Ag-NHC**–**Ag-NHPb** has a small contribution which may come from  $\text{NHE}_{\text{Me}} \rightarrow \text{AgCl}$   $\pi$ -donation and  $\text{NHE}_{\text{Me}} \leftarrow \text{AgCl}$   $\pi$ -back-donation.

Table 2: EDA-NOCV results with interaction energy ( $\Delta E_{int}$ ) and their components ( $\Delta E_{Pauli}$ ,  $\Delta E_{elstat}$ ,  $\Delta E_{orb}$ ) at the BP86/TZ2P+ level for compound **Ag-NHC** – **Ag-NHPb** using the moieties [AgCl] and [ $\text{NHE}_{\text{Me}}$ ] as interacting fragments. The complexes are analyzed with C1 symmetry. All values in kcal/mol

Compound	<b>Ag-NHC</b>	<b>Ag-NHSi</b>	<b>Ag-NHGe</b>	<b>Ag-NHSn</b>	<b>Ag-NHPb</b>
Fragment	AgCl NHC <sub>Me</sub>	AgCl NHSi <sub>Me</sub>	AgCl NHGe <sub>Me</sub>	AgCl NHSn <sub>Me</sub>	AgCl NHPb <sub>Me</sub>
$\Delta E_{int}$	-55.7	-44.6	-34.0	-28.4	-29.5
$\Delta E_{Pauli}$	132.7	117.7	79.8	61.8	48.0
$\Delta E_{elstat}^{[a]}$	-146.2 (77.6 %)	-119.9 (73.9 %)	-79.2 (69.6 %)	-59.7 (66.2 %)	-45.3 (58.4 %)
$\Delta E_{orb}^{[a]}$	-42.2 (22.4 %)	-42.4 (26.1 %)	-34.6 (30.4 %)	-30.5 (33.8 %)	-32.3 (41.6 %)
$\Delta E_{\sigma}^{[b]}$	-29.6 (70.1 %)	-27.8 (65.5 %)	-24.2 (70.0 %)	-22.6 (74.1 %)	-27.6 (85.5 %)
$\Delta E_{\pi}^{[b]}$	-10.4 (24.6 %)	-13.3 (31.3 %)	-9.3 (26.8 %)	-6.7 (22.1 %)	-3.1 (9.5 %)
$\Delta E_{rest}^{[b]}$	-2.2 (5.3 %)	-1.3 (3.2 %)	-1.1 (3.2 %)	-1.2 (3.8 %)	-1.6 (5.0 %)
$\Delta E_{prep}$	0.7	1.3	1.1	1.0	2.0
$\Delta E (= -D_e)^{[c]}$	-55.0 (-57.3) <sup>[c]</sup>	-43.3 (-45.2) <sup>[c]</sup>	-32.9 (-35.1) <sup>[c]</sup>	-27.4 (-27.6) <sup>[c]</sup>	-27.5 (-28.6) <sup>[c]</sup>

<sup>[a]</sup> The relative percentage contributions to the total attractive interaction  $\Delta E_{elstat} + \Delta E_{orb}$

<sup>[b]</sup> The relative percentage contributions to the total orbital interaction  $\Delta E_{orb}$  are given in parentheses

<sup>[c]</sup> The values in parentheses give the dissociation energy at the BP86/def2-TZVPP//BP86/def2-SVP level.

We continue determining the charge transfer between the donor and acceptor fragments by plotting of the pairs of orbitals, the associated deformation densities, and stabilization energies. The  $\Delta E_{orb}$  term was examined of the EDA-NOCV results further in order to obtain more detailed information on the nature of the bonding in **Ag-NHC**–**Ag-NHPb**. The plots of the pairs of orbitals  $\Psi_k/\Psi_k$  that yield the NOCVs providing the largest contributions to the  $\sigma$ - and  $\pi$ -orbital terms  $\Delta E_{\sigma}$  and  $\Delta E_{\pi}$  in **Ag-NHE** (E = C, Pb) and the associated deformation densities  $\Delta\rho$  and stabilization energies are shown in Figure 3. The shape of orbital pairs in **Ag-NHE** (E = Si – Sn) exhibits the head-on mode between  $\text{NHE}_{\text{Me}}$  and AgCl, exhibit similar shapes to those of adduct **Ag-NHC** and therefore, they are not shown in Figure 3. Note that the yellow/blue colors in the figures for  $\Psi_k/\Psi_k$  indicate the sign of the orbitals, and the red/white colors in the deformation density  $\Delta\rho$  designate charge depletion and the white areas point to charge accumulation. The charge flow  $\Delta\rho$  occurs in the direction from red to white. Figures 3 (a) and 3 (c) give the NOCV pairs of  $\sigma$ -orbitals for **Ag-NHC**. The EDA-NOCV results give the effort to understand the nature of chemical bonding in

tetrylene with the nitrogen atoms in  $\text{NHE}_{\text{Me}}$  ring has effects to donor moieties. Figure 3 (a) and 3 (c) shows that the  $\sigma$ -type interaction is clearly from the donating  $\text{NHC}_{\text{Me}}$  fragment to the accepting AgCl fragment. The shapes of the NOCV pairs  $\Psi_2/\Psi_2$  and the deformation density  $\Delta\rho_2$  in Figure 3 (b) show that stabilization of -6.5 kcal/mol can be assigned to  $\text{ClAg} \rightarrow \text{NHC}_{\text{Me}}$   $\pi$ -donation while the stabilization of also comes from the relaxation of the acceptor fragment AgCl in **Ag-NHC**. Figures 3-(d, e, f) show significantly different EDA-NOCV results for **Ag-NHPb** because of the surprising structure of the plumblyene ligand **NHPb**, which is bonded through its  $\pi$ -electron density. Note that the structures and orbitals pairs of the lighter homologues **Ag-NHE** with E = C – Sn have head-on modes between the ligands and AgCl, whereas the heavier species **Ag-NHPb** exhibit a side-on bonded ligands to the AgCl fragment. Figure 3 (d) clearly shows that the  $\sigma$ -type interaction has the direction of the charge flow of  $\text{ClAg} \leftarrow \text{NHPb}_{\text{Me}}$ . The deformation density  $\Delta\rho_1$  exhibits an area of charge donation (red area) at the  $\text{NHPb}_{\text{Me}}$  moiety associated with the deformation density  $\Delta\rho_1$  and stabilization energy is -24.9 kcal/mol. Figures 3 (f) shows that the very weak  $\pi$ -

type orbital interactions in **Ag-NHPb** come from typical  $\pi$ -back-donation  $\text{ClAg} \rightarrow \text{NHPb}_{\text{Me}}$  with the charge flow  $\Psi_3/\Psi_3$  indicates stabilization of -1.5 kcal/mol. Thus, the bonding in the tetrylene complexes **Ag-NHE**<sub>Me</sub> exhibits the typical feature regarding strong  $\sigma$ -donation and weak  $\pi$ -back-donation. From the above results, it can be asserted that the weaker bonds of the heavier complexes  $[\text{AgCl}-\{\text{NHE}_{\text{Me}}\}]$  result from a strong decrease in

the electrostatic component of the W-E bonds. The  $\pi$ -interactions in  $[\text{AgCl}-\{\text{NHE}_{\text{Me}}\}]$  are due to very weak  $\pi$ -back-donation and are also irrelevant for the bond strength. The ligand  $\leftarrow \text{Ag}$   $\pi$ -back-donation in the complexes is very small and the Ag-ligand bonds have a strong ionic character which comes the electrostatic attraction between the positively charged Ag atom and the  $\sigma$ -electron pair of the E donor atom.

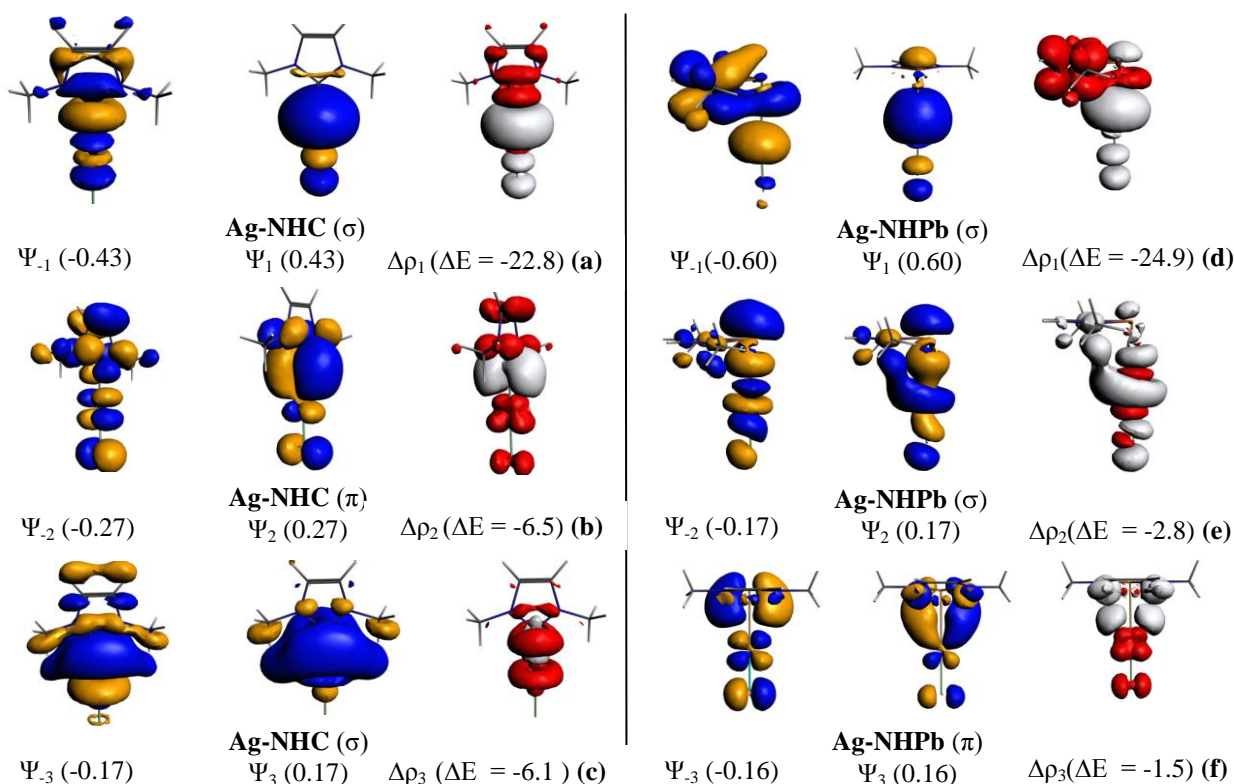


**Figure 3:** Most important NOCV pairs of orbitals  $\Psi_k, \Psi_k$  with their eigenvalues  $-v_{ki}, v_k$  given in parentheses, and the associated deformation densities  $\Delta\rho_k$  and orbital stabilization energies  $\Delta E$  for the complexes **Ag-NHC** and **Ag-NHPb**. The charge flow in the deformation densities is from the red  $\rightarrow$  white region. (a), (c)  $\sigma$ -NOCVs of **Ag-NHC**; (b)  $\pi$ -NOCV of **Ag-NHC**; (d), (e)  $\sigma$ -NOCVs **Ag-NHPb**; (f)  $\pi$ -NOCV of **Ag-NHPb**. Energy values in kcal/mol

#### 4. CONCLUSIONS

DFT calculations find that the equilibrium structures of the **Ag-NHE** show major differences in the bonded orientation of **NHPb** ligand in **Ag-NHPb** compared with **NHE** ligands the slighter homologues **Ag-NHE** (E= C-Sn). The BDE results show that the Ag-carbene bond in **Ag-NHC** is very strong bond and decreases from the slighter to the heavier homologues with the order is **Ag-NHC** > **Ag-NHSi** > **Ag-NHGe** > **Ag-NHSn**  $\approx$  **Ag-NHPb**. Bonding analysis shows that ligands **NHE** exhibit donor-acceptor bonds with the  $\sigma$  lone pair electrons of **NHE** donated into the vacant orbital of the metal fragment AgCl and the ligands **NHE** are strong  $\sigma$ -

donors and very weak  $\pi$  donor and the NOCV pairs of the bonding show small  $\pi$ -back donation from the Ag to the **NHE** ligands. A comprehensive study in the above complexes is needed to give important information to experimentalists about stabilities and properties of as-yet detailed unsynthesized heavier adducts (**Ag-NHSi-Ag-NHPb**).

**Acknowledgements.** *Nguyen Thi Ai Nhung thanks Prof. Dr. Gernot Frenking for allowing the continuous use of her own resources within Frenking's group. The programs of the studies were run via the Erwin/Annemarie clusters operated by Reuti at Philipps-Universität Marburg-Germany. This research is funded by Vietnam National*

Foundation for Science and Technology Development (NAFOSTED) under grant number 104.06-2014.13.

## REFERENCES

1. E. O. Fischer, A. Maasbol. *On the Existence of a Tungsten Carbonyl Carbene Complex*, *Angew. Chem. Int. Ed. Engl.*, **3**, 580-581(1964).
2. D. Nemcsok, K. Wichmann, G. Frenking. *The Significance of  $\pi$  Interactions in Group 11 Complexes with N-Heterocyclic Carbenes*, *Organometallics*, **23**, 3640-3646 (2004).
3. S. Zhu, R. Liang, H. Jiang. *A direct and practical approach for the synthesis of N-heterocyclic carbene coinage metal complexes*, *Tetrahedron*, **68**, 7949-7955 (2012).
4. A. C. Sentman S. Csihony, R. M. Waymouth, J. L. Hedrick. *Silver(I)-Carbene Complexes/Ionic Liquids: Novel N-Heterocyclic Carbene Delivery Agents for Organocatalytic Transformations*, *J. Org. Chem.*, **70**, 2391-2393 (2005).
5. I. J. B. Lin, C. S. Vasam. *Silver(I) N-heterocyclic carbenes*, *Comment. Inorg. Chem.*, **25**, 75-129 (2004).
6. J. C. Garrison, W. J. Youngs. *Ag(I) N-Heterocyclic Carbene Complexes: Synthesis, Structure, and Application*, *Chem. Rev.*, **105**, 3978-4008 (2005). 11
7. A. Kascatan-Nebioglu M. J. Panzner, C. A. Tessier, C. L. Cannon, W. J. Youngs. *N-Heterocyclic carbene-silver complexes: A new class of antibiotics*, *Coord. Chem. Rev.*, **251**, 884-895 (2007).
8. E. C. Hurst K. Wilson, I. J. S. Fairlamb, V. Chechik. *N-Heterocyclic carbene coated metal nanoparticles*, *New J. Chem.*, **33**, 1837-1840 (2009).
9. C. J. Serpell J. Cookson, A. L. Thompson, C. M. Brown, P. D. Beer. *Haloaurate and halopalladate imidazolium salts: structures, properties, and use as precursors for catalytic metal nanoparticles*, *Dalton Trans.*, **42**, 1385-1393 (2013).
10. X. Ling N. Schaeffer, S. Roland, M. Pileni. *Nanocrystals: Why Do Silver and Gold N-Heterocyclic Carbene Precursors Behave Differently?* *Langmuir*, **29**, 12647-12656 (2013).
11. C. K. Lee C. S. Vasam, T. W. Huang, H. M. J. Wang, R. Y. Yang, C. S. Lee, I. J. B. Lin. *Silver(I) N-Heterocyclic Carbenes with Long N-Alkyl Chains*, *Organometallics*, **25**, 3768-3775 (2006).
12. O. Köhl. *Sterically induced differences in N-heterocyclic carbene transition metal complexes*, *Coord. Chem. Rev.*, **253**, 2481-2492 (2009).
13. M. Melaimi, M. Soleilhavoup, G. Bertrand. *Stable Cyclic Carbenes and Related Species beyond Diaminocarbenes*, *Angew. Chem. Int. Ed.*, **49**, 8810-8849 (2010).
14. T. A. N. Nguyen, G. Frenking. *Transition-Metal Complexes of Tetrylones  $[(CO)_5W-E(PPh_3)_2]$  and Tetrylenes  $[(CO)_5W-NHE]$  ( $E = C-Pb$ ): A Theoretical Study*, *Chem. Eur. J.*, **18**, 12733-12748 (2012).
15. T. A. N. Nguyen T. P. L. Huynh, T. X. P. Vo, T. H. Tran, D. S. Tran, T. H. Dang, T. Q. Duong. *Structures, Energies, and Bonding Analysis of Monoaurated Complexes with N-Heterocyclic Carbene and Analogues*, *ASEAN J. Sc. Technol. Dev.*, **32**, 1-15 (2015).
16. C. Boehme, G. Frenking. *N-Heterocyclic Carbene, Silylene, and Germylene Complexes of MCl ( $M = Cu, Ag, Au$ ). A Theoretical Study*, *Organometallics*, **17**, 5801-5809 (1998).
17. C.-Y. Liao K. T. Chan, P. L. Chiu, C. Y. Chen, H. M. Lee. *Structural variation in silver complexes with N-heterocyclic carbene ligands bearing amido functionality*, *Inorg. Chim. Acta.* **361**, 2973-2978 (2008).
18. Y. Inagawa, S. Ishida, T. Iwamoto. *Two-coordinate Dialkylsilylene-Coinage Metal Complexes*, *Chem. Lett.*, **43**, 1665-1667 (2014).
19. N. Zhao J. Zhang, Y. Yang, H. Zhu, Y. Li, G. Fu.  $\beta$ -Diketimate Germylene-Supported Pentafluorophenylcopper(I) and -silver(I) Complexes  $[LGe(Me)(CuC_6F_5)_n]_2$  ( $n = 1, 2$ ),  $LGe[C(SiMe_3)N_2]AgC_6F_5$ , and  $[LGe[C(SiMe_3)N_2](AgC_6F_5)_2]_2$  ( $L = HC[C(Me)N-2,6-iPr_2C_6H_3]_2$ ): Synthesis and Structural Characterization, *Inorg. Chem.*, **51**, 8710-8718 (2012).
20. P. B. Hitchcock M. F. Lappert, L. J. M. Pierssens. *Novel  $Sn^{II}-Ag^I$  Reactions from  $Sn[CH(SiMe_3)_2]_2$  and  $AgX$  ( $X = NCS, CN, NCO, or I$ ):  $Sn^{II}-Ag^I$  or  $Sn^{IV}X_2$  Complexes*, *Organometallics*, **17**, 2686-2688 (1998).

Corresponding author: **Nguyen Thi Ai Nhung**

Hue University of Sciences, Hue University  
No. 77, Nguyen Hue, Hue City, Thua Thien Hue Province  
E-mail: nguyennainhung.hueuni@gmail.com.